



Lawrence Berkeley Laboratory

UNIVERSITY OF CALIFORNIA

RECEIVED
LAWRENCE
BERKELEY LABORATORY

FEB 18 1986

LIBRARY AND
DOCUMENTS SECTION

Materials & Molecular Research Division

Presented at the 1985 Fall Materials Research
Meeting, Symposium A, Boston, MA,
November 30-December 2, 1984

NONLINEAR OPTICS AND SURFACE SCIENCE

Y.R. Shen

November 1985

TWO-WEEK LOAN COPY
*This is a Library Circulating Copy
which may be borrowed for two weeks.*



LBL-20064
e.2

DISCLAIMER

This document was prepared as an account of work sponsored by the United States Government. While this document is believed to contain correct information, neither the United States Government nor any agency thereof, nor the Regents of the University of California, nor any of their employees, makes any warranty, express or implied, or assumes any legal responsibility for the accuracy, completeness, or usefulness of any information, apparatus, product, or process disclosed, or represents that its use would not infringe privately owned rights. Reference herein to any specific commercial product, process, or service by its trade name, trademark, manufacturer, or otherwise, does not necessarily constitute or imply its endorsement, recommendation, or favoring by the United States Government or any agency thereof, or the Regents of the University of California. The views and opinions of authors expressed herein do not necessarily state or reflect those of the United States Government or any agency thereof or the Regents of the University of California.

Y. R. SHEN

Department of Physics, University of California, Berkeley, California and
Materials and Molecular Research Division, Lawrence Berkeley Laboratory,
Berkeley, California 94720

ABSTRACT

The recent status of applications of nonlinear optics to surface science is reviewed. The basic theory of wave mixing on a surface layer, and the possibility of using various nonlinear optical processes for surface probing are briefly discussed. Emphasis is on surface second harmonic generation, which is shown with many illustrations to be a rather unique and versatile tool for surface studies.

INTRODUCTION

In recent years, laser applications to surfaces have created much excitement and many unique opportunities in surface science and technology [1]. On the other hand, numerous laser techniques have been invented for surface material processing. Laser annealing, alloying, ablation, and photochemical etching or deposition are among the well-known examples. On the other hand, novel laser methods have been developed for surface probing. These include photoacoustic [2], photothermal [3], and photodesorption [4] spectroscopy, as well as state-selective detection of molecules collided with or desorbed from a surface [5]. The recent advances in the applications of nonlinear optical techniques to material studies have naturally brought our attention to the possible applications of nonlinear optics to surfaces. One might question whether nonlinear optical techniques are sensitive enough for surface probing. Actually, the surface sensitivity of nonlinear optical effects was already demonstrated more than 15 years ago [6], but applications of nonlinear optics to surface probing were only recently realized [7].

As optical probes, nonlinear optical techniques have many intrinsic merits. They are nondestructive, capable of in-situ remote sensing with high spatial and temporal resolution, and applicable to any interface accessible by light. In comparison with linear optical methods, nonlinear optical techniques have the further advantages of being more versatile and more surface sensitive and specific. The nonlinear signal usually increases with increasing pump laser intensity, but is limited eventually by optical damage. As we shall see later, submonolayers of adsorbates on a surface are often readily detectable by the nonlinear techniques [7].

The nonlinear optical effects that are capable of probing surfaces via measurements of their optical properties generally fall into the class of wave mixing. Both four-wave mixing and three-wave mixing (including second harmonic generation) have been considered as viable surface probes. The former has the advantage that a wide range of resonances can be resonantly excited and probed [8]. However, being a third-order effect, it suffers from a relatively weak signal strength and a poor discrimination of surface against bulk. Three-wave mixing could discriminate surface against bulk and yields a fair signal, but its spectroscopic capability is severely limited by the existing laser tuning range.

In the following, we shall first briefly review the basic understanding of surface nonlinearity and associated surface nonlinear optics, and then describe the applications of various nonlinear optical effects to surface studies.

The abrupt termination of a bulk at a surface makes the surface layer structurally very different from the bulk. Consequently, the surface and bulk are expected to have significantly different optical properties. In addition, the normal component of an optical field varies rapidly across the surface layer such that the response of the surface layer to the field is extremely nonlocal. All these indicate that the surface layer should be characterized by a different set of optical constants than the bulk.

We can define the surface layer as the layer where both the structure of the medium and the optical field vary significantly [9]. It is well-known that such a variation generally occurs in a distance of few atomic or molecular layers. Thus, the surface layer thickness is always much smaller than an optical wavelength. As a result, in discussing optical effects resulting from the optical response of the surface layer, we can treat the layer as infinitely thin. We can then use an n th-order surface nonlinear susceptibility $\vec{\chi}_S^{(n)}$ to describe the n th-order surface polarization $\vec{P}_S^{(n)}$ induced in the surface layer [9].

$$P_{S,i}^{(n)}(\omega = \omega_1 + \dots + \omega_n) = \chi_{S,ij_1\dots j_n} F_{j_1}(\omega_1) \dots F_{j_n}(\omega_n)$$

$$F_j = E_j \quad \text{if } j = x, y$$

$$= D_j \quad \text{if } j = z \quad (1)$$

assuming $\hat{x} - \hat{y}$ is the surface plane. Here, E and D denote the electric field and displacement current, respectively. Since both the parallel field and the normal displacement current components are continuous across the surface layer, $\vec{\chi}_S^{(n)}$ so defined is unique, unaffected by the different values of the normal field components on the two sides of the layer.

As it stands, $\vec{\chi}_S^{(n)}$ appears as a local quantity, although it contains all the nonlocal response of the surface layer. Symmetry of the surface layer dictates the symmetric form of $\vec{\chi}_S^{(n)}$. Because the inversion symmetry is necessarily broken at a surface, the second-order susceptibility $\vec{\chi}_S^{(2)}$ is nonvanishing even if $\vec{\chi}^{(2)}$ vanishes in the bulk under the electric-dipole approximation. This result is a clear indication of the surface specificity of the second-order processes.

The various components of $\vec{\chi}_S^{(n)}$ for a surface layer can in principle be obtained from measurements of nonlinear reflection at the surface, as will be discussed in the next section. Typically, $\vec{\chi}_S^{(2)}$ is of the order of $10^{-14} - 10^{-16}$ esu and $\vec{\chi}_S^{(3)}$ is of the order of $10^{-20} - 10^{-23}$ esu. How $\vec{\chi}_S^{(n)}$ is related to the microscopic structure of the surface layer is of course a matter of great concern. Unfortunately, the theory is not yet well developed, and the limited understanding depends very much on the particular system under consideration.

NONLINEAR OPTICAL GENERATION FROM A SURFACE

We consider the system in Fig. 1. The plane interface at $z = 0$ is formed by an isotropic medium at $z < 0$ and vacuum at $z > 0$. Laser excitation of the medium induces a bulk nonlinear polarization $\vec{P}_V^{(n)} = \vec{\mathcal{P}}_V^{(n)} \times \exp(iK_x x + iK_z z - i\Omega t)$ in the bulk and a surface nonlinear polarization $\vec{P}_S^{(n)} = \vec{\mathcal{P}}_S^{(n)} \exp(iK_x x - i\Omega t)$ on the surface. We are interested in the output generated by $\vec{P}_V^{(n)}$ and $\vec{P}_S^{(n)}$ on the vacuum side.

The wave equation for the output field takes the form

$$[\nabla^2 + (\frac{\Omega}{c})^2 \epsilon] \vec{E}(\Omega) = -4\pi(\frac{\Omega}{c})^2 [\vec{P}_S^{(n)} \delta(z) + \vec{P}_V^{(n)}]. \quad (2)$$

The solution of this equation has been obtained in various forms by differ-

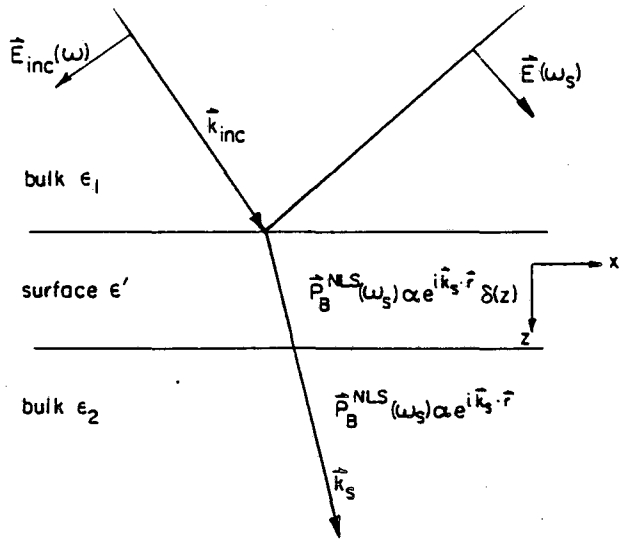


Fig. 1 An interface system with a surface nonlinear polarization $\vec{P}_S^{(n)}$ and a bulk nonlinear polarization $\vec{P}_V^{(n)}$.

ent authors [10,11]. We find

$$E_y(\Omega) = \frac{i4\pi(\Omega/c)^2}{K_{1z} + K_{2z}} \left[\mathcal{P}_{Sy}^{(n)} - \frac{\mathcal{P}_{Vy}^{(n)}}{K_{sz} + K_{2z}} \right] e^{i\vec{k}_1 \cdot \vec{r} - i\Omega t}$$

$$E_x(\Omega) = (K_{1z}/K_x) E_z(\Omega)$$

$$= \frac{i4\pi K_{1z} K_{2z}}{K_{2z} + \epsilon_2 K_{1z}} \left[\mathcal{P}_{Sx}^{(n)} + \frac{\epsilon_2 K_x}{K_{2z}} \mathcal{P}_{Sz}^{(n)} + i \frac{K_{2z} \mathcal{P}_{Vx}^{(n)} - K_x \mathcal{P}_{Vz}^{(n)}}{K_{2z} (K_{sz} + K_{2z})} \right], \quad (3)$$

where \vec{k}_1 and \vec{k}_2 denote the wavevectors of the free waves at frequency Ω in media 1 and 2, respectively, with $K_{1x} = K_{2x} = K_{sx} \equiv K_x$.

It is readily seen, from Eq. (3), that both surface and bulk nonlinear polarizations contribute to the output. For $(K_{sz} + K_{2z}) \sim K_2$, the ratio of the two contributions to $E(\Omega)$ is of the order of $(2\pi/\lambda) |\mathcal{P}_S^{(n)}| / |\mathcal{P}_V^{(n)}|$ [11]. If the surface layer has a structure not very different from the bulk, we expect $|\mathcal{P}_S^{(n)}| \sim |\mathcal{P}_V^{(n)}| d$, where d is the surface layer thickness, then the ratio becomes $2\pi(d/\lambda)$ which is much less than 1. The output signal would completely be dominated by the bulk contribution unless one could resort to special techniques to enhance the surface contribution and/or suppress the bulk contribution. This is the case with four-wave mixing and with three-wave mixing in noncentrosymmetric media. In the case of a centrosymmetric medium, the second-order bulk polarization $P_V^{(2)}$ is zero in the electric dipole approximation. It is nonzero only if electric-quadrupole and magnetic-dipole contributions are taken into account, but is reduced by a factor of $\sim 2\pi a/\lambda$ in comparison with that for a noncentrosymmetric medium, where a denotes the atomic size. The ratio of surface contribution to bulk contribution in this case becomes [11] $\sim (2\pi/\lambda)[d/(2\pi a/\lambda)] = d/a > 1$. The surface contribution can be significantly modified by the presence of adsorbates, as we shall see. With special arrangement of beam polarizations and directions, it is also possible to yield a vanishing $P_V^{(2)}$ so that only the surface is responsible for the nonlinear output [9].

Assuming that $\vec{P}_S^{(n)}$ can be separately deduced from the measurements, we can then obtain $\vec{P}_V^{(n)}$ from the results using Eq. (1). The approximate output signal from $\vec{P}_S^{(n)}$ can be calculated from Eq. (3). We find

$$S(\Omega) \sim (4\pi\Omega/c\lambda) |\mathcal{P}_S^{(n)}|^2 A T \text{ photons/pulse}, \quad (4)$$

where A is the beam cross-section on the surface and T is the pulsewidth.

In many cases, we may be interested only in the change due to surface modification such as adsorption of molecules to the surface. Relative measurements to deduce $\Delta\chi_S^{(n)}$ are always much simpler and more straightforward.

SURFACE COHERENT RAMAN SPECTROSCOPY

Among the many possible four-wave mixing processes, we shall consider only coherent Raman effects here because they are potentially useful as spectroscopic tools for surface analysis [11]. In the so-called antiStokes Raman scattering (CARS) [8], two incident laser beams at frequencies ω_1 and ω_2 induce a nonlinear polarization $\vec{P}^{(3)}(\Omega = 2\omega_1 - \omega_2)$ in a medium. If $\omega_1 - \omega_2$ is near a Raman resonance at ω_V , then $\vec{P}^{(3)}$ is resonantly enhanced. The corresponding $\chi^{(3)}$ can be decomposed into a resonant and nonresonant part

$$\chi^{(3)}(\Omega = 2\omega_1 - \omega_2) = \chi_R^{(3)} + \chi_{NR}^{(3)}$$

$$\chi_R^{(3)} = A/[(\omega_1 - \omega_2) - \omega_{ex} + i\Gamma_{ex}]. \quad (5)$$

Thus, by scanning $(\omega_1 - \omega_2)$ and observing the resonant enhancement of the output at Ω , we can learn about the Raman resonance. The very attractive feature of this technique is that an extremely wide range of $(\omega_1 - \omega_2)$, from 0 to $\sim 10^5 \text{ cm}^{-1}$, can be easily covered by beating a tunable dye laser with a fixed-frequency laser.

Obviously, CARS should also be applicable to surfaces. The difficulty lies in the strong bulk contribution to the signal. As a third-order nonlinear effect, there is no intrinsic symmetry rule that discriminates a surface from a bulk. Although $\vec{\chi}_S^{(3)}$ may have a different resonant spectrum than $\vec{\chi}_V^{(3)}$, spectral discrimination by the detection system to suppress the bulk contribution is often not sufficient. Polarization discrimination must be used in addition to further reduce the bulk contribution. This is based on the fact that $(\vec{\chi}_S^{(3)})_R$ generally yields an output polarized in a different direction than $\vec{\chi}_V^{(3)}$ and $(\vec{\chi}_S^{(3)})_{NR}$. There is also the question whether the output signal from $(\vec{\chi}_S^{(3)})_R$ is strong enough to be detected. Using $(\vec{\chi}_S^{(3)})_R \sim 10^{-20}$ esu and picosecond excitation pulses with $I \sim 10^{10} \text{ W/cm}^2$, $T \sim 1 \text{ psec}$, and $A \sim 0.1 \text{ cm}^2$ in Eq. (4), we find $S \sim 10^3$ photons/pulse, which should be easily detectable.

The surface CARS signal can be greatly enhanced if surface [12] or guided [13] optical waves are used to enhance the pump laser intensity and the effective interaction length. This has been demonstrated experimentally. The disadvantage of such a scheme is that the polarization discrimination method is not easily applicable [13].

Another coherent Raman technique which automatically eliminates the nonresonant surface and bulk contribution is stimulated Raman gain spectroscopy [14]. The input beams are again at ω_1 and ω_2 with $(\omega_1 - \omega_2) \sim \omega_{ex}$, but the output resulting from the induced $\vec{P}^{(3)}(\omega_2 = \omega_1 - \omega_1 + \omega_2)$ is measured as a change superimposed on the input $E(\omega_2)$. Assuming that only $(\chi_S^{(2)})_R$ is resonant at $(\omega_1 - \omega_2) \sim \omega_{ex}$, one would find

$$\Delta|E(\omega_2)|^2 = G|E(\omega_2)|^2$$

$$G = (4\pi\omega_2/c)\text{Im}(\chi_S^{(2)})_R|E(\omega_1)|^2. \quad (6)$$

If $\text{Im}(\chi_S^{(2)})_R \sim 10^{-20}$ esu and $I \sim 10^9 \text{ W/cm}^2$, we find $G \sim 5 \times 10^{-8}$. It has been demonstrated that with CW mode-locked laser pulses and a synchronous detection system, G as small as 10^{-8} can be detected. Therefore, surface Raman spectra are indeed measurable [14]. Unfortunately, the limited laser intensity, the residual adsorption of the substrate, and the limited sta-

bility of the laser and detection systems make the measurements quite difficult.

SURFACE SECOND HARMONIC GENERATION

As we mentioned earlier, second-order nonlinear effects favor the surface against the bulk in a medium with inversion symmetry. It is therefore ideal as a tool for surface studies. Second harmonic generation (SHG) is particularly attractive because of the simplicity in the experimental arrangement, as shown in Fig. 2. Unlike the third-order effects, the signal

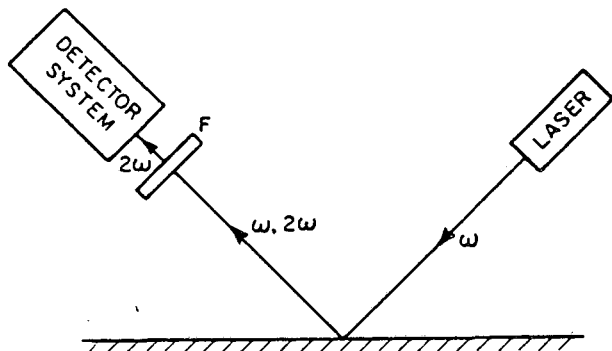


Fig. 2 Experimental arrangement for second harmonic generation from a surface.

from SHG is generally much stronger [11]. Even without resonance, $\chi_S^{(2)}$ can be as large as $\sim 10^{-15}$ esu. Using Eq. (4) with $I \sim 10^{10}$ W/cm², $T \sim 1$ psec, and $A \sim 0.1$ cm², we find $S \sim 4 \times 10^5$ photons/pulse. With $T \sim 10$ nsec, $I \sim 10^6$ W/cm², and $A \sim 1$ cm, we still have $S \sim 400$ photons/pulse. The signal is actually only limited by optical damage. It then happens that because of the higher energy damage threshold in the CW case, even a CW laser is intense enough for generating detectable SHG from a surface monolayer. In a recent experiment using a 20-mV CW diode laser, we could indeed use SHG to monitor adsorption and desorption of monolayers of molecules on an electrode in an electrolytical cell [15].

In the past several years, it has been firmly established that SHG is a viable tool for surface studies. The technique has been successfully applied to many different surfaces and interfaces to study either bare surface properties or molecular adsorbates. We describe here a few representative cases to illustrate the broad range of applications of the technique.

Surface SHG can be used to study bare surfaces [16]. A freshly cleaved Si(111) surface is known to reconstruct to form a (2×1) structure. Annealing changes it into (7×7) . The (2×1) structure should yield a 2-fold rotational symmetry in the SHG about the surface normal, while the (7×7) structure should lead to an isotropic variation. This was indeed observed by Heinz et al. [16], as shown in Fig. 3. The result confirmed the π -bonded chain model description for the (2×1) -Si(111) surface. A real time monitoring of the surface transformation from (2×1) to (7×7) structure during annealing was also possible using SHG. In this case, with the selected polarization combination, the bulk contribution to the SH signal was negligible. Surface melting can also be monitored by SHG [17]. Using fsec-laser pulses, it was found that the laser-induced melting of Si(111) takes place in ~ 1 psec. Aside from probing surface symmetry, SHG should also be useful for spectroscopic studies of surface states.

Surface SHG is generally more useful for studies of adsorbates at an interface. A monolayer of adsorbates changes the surface susceptibility from its bare value $\chi_S^{(2)}$ to the modified value $\chi_S^{(2)}$, with

$$\chi_S^{(2)} = \chi_S^{(2)} + \chi_{AS}^{(2)} + \chi_A^{(2)}$$

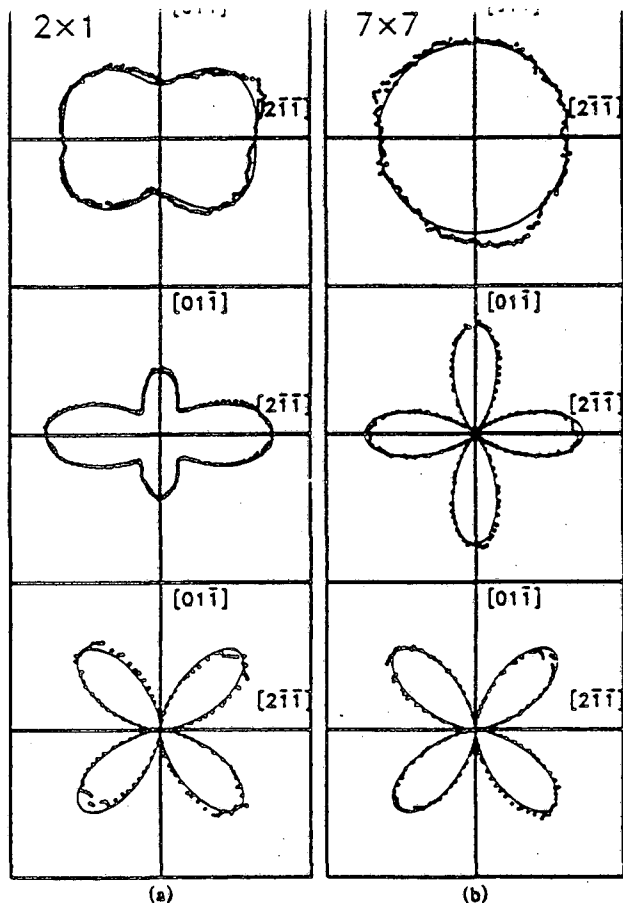


Fig. 3 SH intensity from Si(111)-(2 x 1) and (7 x 7) surfaces as a function of pump polarization. Different curves correspond to different SH polarizations. See Ref. 16.

where $\chi_{AS}^{(2)}$ and $\chi_A^{(2)}$ denote, respectively, the susceptibility changes arising from the adsorbate/surface interaction and from the intrinsic nonlinearity of the layer of adsorbates. If the interaction between adsorbate molecules is negligible, then both $\chi_{AS}^{(2)}$ and $\chi_A^{(2)}$ are proportional to the surface density of adsorbate molecules, N/cm^2 . Typically, for metal and semiconductor surfaces, $\chi_S^{(2)} \sim 10^{-14}$ esu, which is quite appreciable. A monolayer of atoms or molecules chemisorbed on metal or semiconductor is expected to yield a $\chi_{AS}^{(2)}$, which is an appreciable fraction of $\chi_S^{(2)}$, and therefore should be easily detectable even if $\chi_A^{(2)}$ is small. On the other hand, for insulators, $\chi_S^{(2)} \sim 10^{-15}$ esu is relatively small, and $\chi_{AS}^{(2)}$ is often even smaller. A monolayer of molecular adsorbates is detectable only if the intrinsic nonlinearity of the molecules, $\chi_A^{(2)}$, is sufficiently large.

Indeed, experiments showed that even submonolayers of adsorbates on metals [18,19] and semiconductors [19] are easily detectable. A number of examples are given in Figs. 4-6. These are results obtained from well defined sample surfaces in ultrahigh vacuum. Figure 4 describes how the SH signal from Ni(111) varies with surface exposure to CO [19]. Adsorption of CO on Ni(111) is known to be on sites of the same type, and hence the adsorption kinetics could obey the simple Langmuir model. The data in Fig. 4 are indeed in excellent agreement with prediction from the Langmuir model. In the case of CO adsorption on Rh(111) [18], the result in Fig. 5 shows that the variation of the SHG with CO coverage θ , as calibrated by LEED, exhibits a sudden change in slope at $\theta = 1/3$ monolayer. This agrees with the fact that for $\theta < 1/3$, only adsorption sites of a single type can be occupied by CO on Rh(111), but for $1/3 \leq \theta < 3/4$, new sites of a different type also becomes open for CO adsorption. The data in Fig. 5 can actually be described very well by such a two-site model. Oxidation of a semiconductor surface can also be monitored by SHG [20]. Figure 6 shows the results obtained from Si(111). The decrease in the SH signal is dominated by the adsorption of the first monolayer of oxygen on Si, and can be fit by

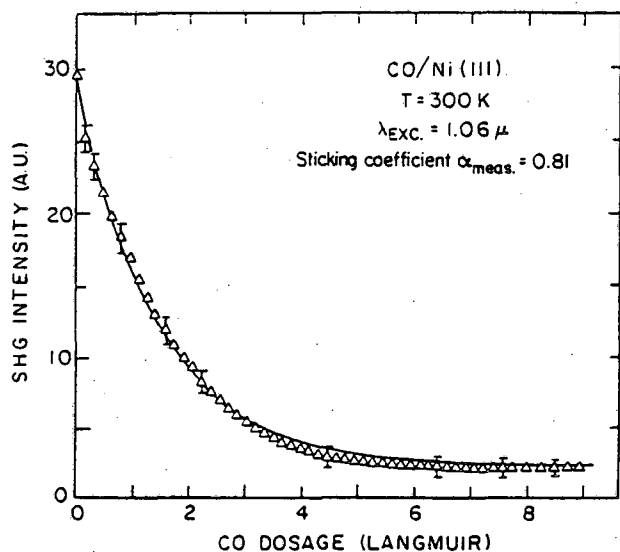


Fig. 4 SH signal as a function of surface coverage of CO on Ni(111) at 300K. The solid theoretical curve derived from the Langmuir kinetic model is used to fit the data.

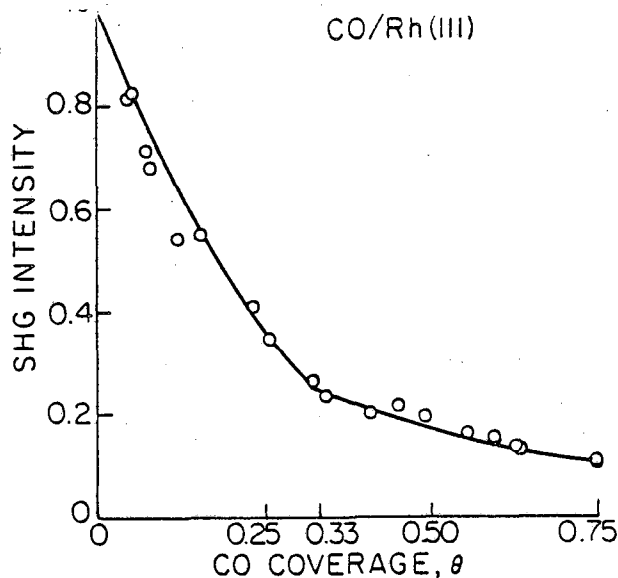


Fig. 5 SH signal from CO/Rh(111) as a function of CO fractional coverage. The solid curve is a theoretical fit.

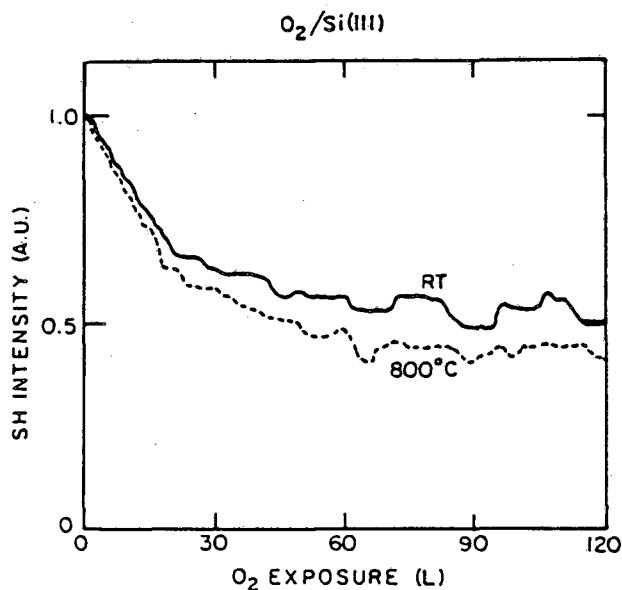


Fig. 6 SHG from Si(111) during oxidation of the surface at room temperature (RT) and at 800°C (---).

the simple Langmuir model assuming a single type of adsorption site, as indicated in Fig. 6. In all the cases presented here, the SH signal appears to decrease with increase of surface coverage of adsorbates. This is however not generally true. It depends on the adsorbate/surface interaction which dictates the relative sign of $\chi_{\text{S}}^{(2)}$ and $\chi_{\text{AS}}^{(2)}$. For example, adsorption of alkali atoms on metals would actually lead to a strong increase in the surface SHG [18].

As a tool to monitor adsorbates, one may need to calibrate the SH signal for absolute measurement of surface coverage of adsorbates. This can be done by correlating the SH signal with the results from thermal desorption spectroscopy (TDS) [19]. In comparison with TDS and other surface probes, SHG has the advantage of being almost instantaneous in response. It therefore could be an ideal tool for studies of surface dynamics.

Adsorption of molecules on insulator surfaces can also readily be de-

ected by SHG, although the sensitivity is relatively low if the molecules are not highly nonlinear. This has been demonstrated in a number of cases [15,21-24]. An example is given in Fig. 7, where it is shown that a small hole in a monolayer of rhodamine 6G molecules adsorbed on fused quartz can be clearly observed by SHG [15]. The technique is therefore potentially useful for surface microscopy. With a better focusing lens, a spatial resolution close to 1 μm should be achievable.

Spectroscopy of molecular adsorbates is also possible with surface SHG [21]. Figure 8 shows the spectra of the $S_0 \rightarrow S_2$ transition of half monolayers of rhodamine 6G and rhodamine 110 on fused quartz. The spectral lines of the two dye molecules are well resolved even though structurally the two molecules are quite similar. This indicates that SHG can be used to identify or distinguish different adsorbates on a surface.

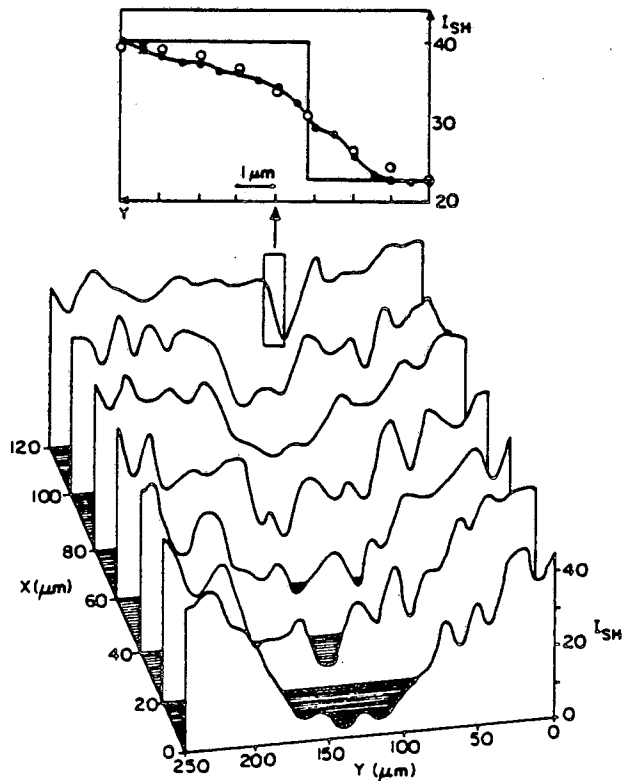


Fig. 7 SH image of an ablated hole in a Rhodamine 6G dye monolayer. Insert: a high resolution scan of the region bracketed by the rectangle.

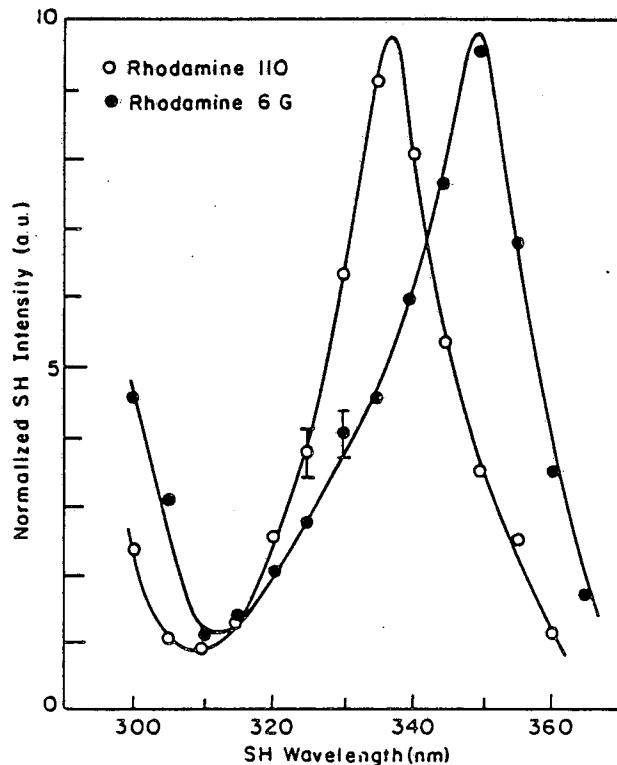


Fig. 8 SH spectra of the $S_0 \rightarrow S_2$ transition for submonolayers of rhodamine 6G and 110 dye molecules adsorbed on fused silica.

Surface SHG is rather unique as a tool that is applicable to essentially all interfaces. For example, it has been used to study molecules at liquid/solid [22] and air/liquid [23] interfaces. Figure 9 shows the adsorption isotherm of p-nitrobenzoic acid (PNBA) on fused quartz from an ethanol solution obtained by SHG [22]. From the adsorption isotherm, the adsorption free energy of - 8 KCal/mole can be deduced. Time-dependent measurement of adsorption and desorption of molecules at a liquid/solid interface is also possible.

When the intrinsic molecular nonlinearity $\chi_A^{(2)}$ dominates in the surface nonlinear susceptibility $\chi_S^{(2)}$ or can be extracted from $\chi_S^{(2)}$, surface SHG with different polarization combinations can yield information about the orientation of molecules on a surface [22]. This is because $\chi_A^{(2)}$ in the lab coordinates is related to the nonlinear polarizability $\alpha^{(2)}$ of the molecules by a simple coordinate transformation assuming negligible interac-

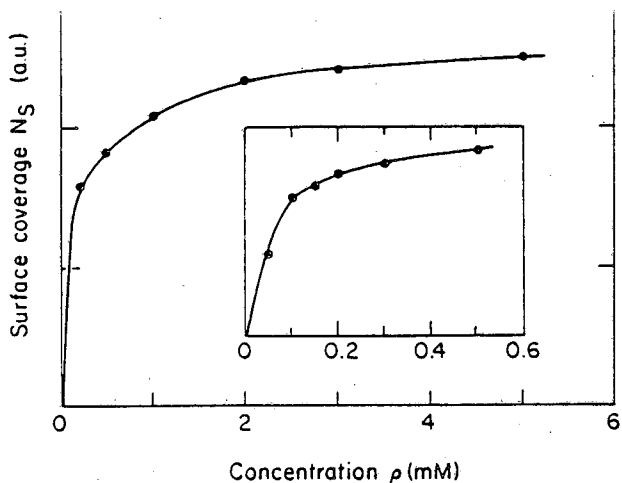


Fig. 9 Adsorption isotherm of PNBA on fused quartz out of an ethanol solution as deduced from SHG.

tion between molecules. We illustrate it with the simple case where $\alpha^{(2)}$ is dominated by a single element $\alpha_{\xi\xi\xi}^{(2)}$ along a molecular coordinate ξ , and the molecules are arranged with an azimuthal symmetry. Then one can easily show that

$$\begin{aligned} (\chi_A^{(2)})_{zzz} &= N \langle \cos^3 \theta \rangle \alpha_{\xi\xi\xi}^{(2)} \\ (\chi_A^{(2)})_{zxx} &= (\chi_A^{(2)})_{xzx} = \frac{1}{2} N \langle \cos \theta \sin^2 \theta \rangle \alpha_{\xi\xi\xi}^{(2)}, \end{aligned} \quad (7)$$

where θ is the angle $\hat{\xi}$ makes with the surface normal \hat{z} . The weighted average orientation of the molecules, $\langle \cos^3 \theta \rangle / \langle \cos \theta \sin^2 \theta \rangle$, can be deduced from the ratio of the measured $(\chi_A^{(2)})_{zzz}$ and $(\chi_A^{(2)})_{zxx} + (\chi_A^{(2)})_{xzx}$. The method has been applied to different molecules at various interfaces [22-24].

Application of the above technique to pentadecanoic acid molecules floating on a water surface led to the result in Fig. 10 [24]. It is seen

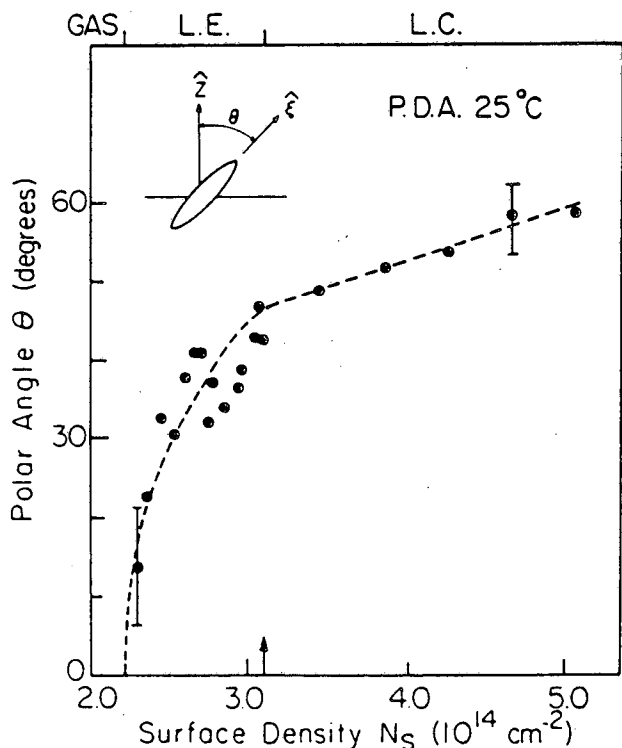


Fig. 10 Tilt angle θ between the molecular axis and the surface normal as a function of surface density of PDA on water at 25°C.

that at the surface density where the so-called liquid-expanded to liquid-compressed phase transition first takes place, the slope of molecular ori-

entation versus surface density changes suddenly. Analysis of the result in Fig. 10 shows that the phase transition must be of first-order and the two phases differ not only by a density change but also by a change in the molecular orientation.

There are many other possible applications of surface SHG one can think of. Studies of surface dynamics, polymerization, and catalytical reactions are just a few examples. The strength of the technique clearly lies in its great time-resolving capability and applicability to the large variety of interfaces.

SURFACE SUM-FREQUENCY GENERATION

The major shortcoming of SHG as a surface analytical tool is its poor spectral selectivity. The electronic transitions that SHG can probe are often too broad to be useful for distinguishing species with similar structures. The vibrational transitions can better characterize molecular species, but surface SHG in the infrared is difficult to detect because of insensitivity of infrared photodetectors. A possible solution is to employ, instead of SHG, infrared-visible sum-frequency generation. A tunable infrared laser is used to probe the vibrational transitions and the resonances are displayed in the visible by up-conversion. Such a scheme is presently being attempted.

OTHER NONLINEAR OPTICAL TECHNIQUES

A number of other nonlinear optical effects have been employed for surface studies. They are however not all-optical methods. Multiphoton ionization has been used to map out the energy distribution in molecules after collision with or desorption from a surface [5]. Multiphoton photoemission has been used to probe the surface states of semiconductors [25]. Finally, infrared multiphoton absorption of molecular adsorbates on a surface could lead to desorption of the molecules, and can therefore be used as a surface spectroscopy technique [4].

CONCLUDING REMARKS

Applications of nonlinear optical techniques to surface studies are still in the developing stage. However, it is already obvious that they possess some advantages unique among conventional surface techniques. The possibility of studying surface dynamics with ultrashort laser pulses is one example. As complementary tools to the existing surface probes, the nonlinear optical techniques are likely to bring surface science into a new dimension.

ACKNOWLEDGEMENT

This work was supported by the Director, Office of Energy Research, Office of Basic Energy Sciences, Materials Sciences Division of the U.S. Department of Energy under Contract No. DE-AC03-76SF00098.

REFERENCES

1. See, for example, Surface Studies with Lasers, eds. F. R. Aussenegg, A. Leitner, and M. E. Lippitsch (Springer-Verlag, Berlin, 1983); papers presented in Topical Meeting on Microphysics on Surfaces, Beams,

- and adsorbates (Santa Fe, February, 1985) (to be published in J. Vac. Sci. Techn. B).
2. F. Trager, H. Coufal, and T. J. Chuang, Phys. Rev. Lett. 49, 1720 (1982).
 3. A. C. Boccara, D. Fournier, and J. Badoz, Appl. Phys. Lett. 36, 130 (1980); M. A. Olmstead and N. M. Amer, Phys. Rev. Lett. 52, 1148 (1984).
 4. T. J. Chuang and H. Seki, Phys. Rev. Lett. 49, 382 (1982).
 5. See, for example, H. Zacharias, M. M. T. Loy, and P. A. Roland, Phys. Rev. Lett. 49, 1790 (1982); J. Haeger, Y. R. Shen, and H. Walther, Phys. Rev. A 31, 1962 (1984); and references therein.
 6. F. Brown, R. E. Parks, and A. M. Sleeper, Phys. Rev. Lett. 14, 1029 (1965); N. Bloembergen, R. K. Chang, and C. H. Lee, Phys. Rev. Lett. 16, 986 (1966); N. Bloembergen, R. K. Chang, S. S. Jha, and C. H. Lee, Phys. Rev. 174, 813 (1968); C. C. Wang and A. N. Duminski, Phys. Rev. Lett. 20, 668 (1968); F. Brown and R. E. Parks, Phys. Rev. Lett. 16, 507 (1966); J. M. Chen, J. R. Bower, C. S. Wang, and C. H. Lee, Optics Commun. 9, 132 (1973).
 7. See, for example, T. F. Heinz, H. W. K. Tom, and Y. R. Shen, Laser Focus 19, 101 (1983).
 8. See, for example, Y. R. Shen, The Principles of Nonlinear Optics (J. Wiley, New York, 1984), Chapter 15.
 9. P. Guyot-Sionnest, W. Chen, and Y. R. Shen (to be published).
 10. N. Bloembergen, R. K. Chang, S. S. Jha, and C. H. Lee, Phys. Rev. 174, 813 (1968); C. C. Wang, Phys. Rev. 178, 1457 (1969).
 11. Y. R. Shen, The Principles of Nonlinear Optics (J. Wiley, New York, 1984), Chapter 25.
 12. C. K. Chen, A. R. B. de Castro, Y. R. Shen, and F. DeMartini, Phys. Rev. Lett. 43, 946 (1979).
 13. W. M. Hetherington, N. E. Van Wyck, E. W. Koenig, G. I. Stegeman, and R. M. Fortenberry, Optics Lett. 9, 89 (1984); J. Chem. Phys. (to be published).
 14. J. P. Heritage and D. L. Allara, Chem. Phys. Lett. 74, 507 (1980).
 15. G. T. Boyd, Y. R. Shen, and T. W. Hansch (submitted to Optics Lett.)
 16. T. F. Heinz, M. M. T. Loy, and W. A. Thompson, Phys. Rev. Lett. 54, 63 (1985).
 17. C. V. Shang, R. Yen, and C. Hirlimann, Phys. Rev. Lett. 51, 900 (1983); S. A. Akhmanov, N. I. Koroteev, G. A. Paitian, I. L. Shumay, M. F. Galjautdinov, I. B. Khaibullin, and E. I. Shtyrkov, Optics Commun. 47, 202 (1983); J. Opt. Soc. Am. B 2, 283 (1985); A. M. Malvezzi, J. M. Lire, and N. Bloembergen, Appl. Phys. Lett. 45, 1019 (1984).
 18. H. W. K. Tom, C. M. Mate, X. D. Zhu, J. E. Crowell, T. F. Heinz, G. Somorjai, and Y. R. Shen, Phys. Rev. Lett. 52, 348 (1984).
 19. X. D. Zhu, R. Carr, and Y. R. Shen, Surf. Sci. (to be published).
 20. H. W. K. Tom, X. D. Zhu, Y. R. Shen, and G. A. Somorjai, Proc. XVII Internatl. Conf. on Physics of Semiconductors (Springer-Verlag, Berlin, 1984), p.99; T. F. Heinz, M. M. T. Loy, and W. A. Thompson, J. Vac. Soc. Tech. (to be published).
 21. T. F. Heinz, C. K. Chen, D. Ricard, and Y. R. Shen, Phys. Rev. Lett. 48, 478 (1982).
 22. T. F. Heinz, H. W. K. Tom, and Y. R. Shen, Phys. Rev. A 28, 1883 (1983).
 23. Th. Rasing, Y. R. Shen, M. W. Kim, P. Valint, and J. Bock, Phys. Rev. A 31, 537 (1985).
 24. Th. Rasing, Y. R. Shen, M. W. Kim, and S. Grubb (to be published).
 25. R. Haight, J. Bokor, J. Stark, R. H. Storz, R. R. Freeman, and P. H. Bucksbaum, Phys. Rev. Lett. 54, 1302 (1985).

This report was done with support from the Department of Energy. Any conclusions or opinions expressed in this report represent solely those of the author(s) and not necessarily those of The Regents of the University of California, the Lawrence Berkeley Laboratory or the Department of Energy.

Reference to a company or product name does not imply approval or recommendation of the product by the University of California or the U.S. Department of Energy to the exclusion of others that may be suitable.

*LAWRENCE BERKELEY LABORATORY
TECHNICAL INFORMATION DEPARTMENT
UNIVERSITY OF CALIFORNIA
BERKELEY, CALIFORNIA 94720*